Journal of Physiology (2002), **545.1**, *pp.* 13–26
DOI: 10.1113/jphysiol.2002.027052

www.jphysiol.org

Interaction with 14-3-3 proteins promotes functional expression of the potassium channels TASK-1 and TASK-3

Sindhu Rajan *, Regina Preisig-Müller *, Erhard Wischmeyer *†, Ralf Nehring †, Peter J. Hanley, Vijay Renigunta, Boris Musset, Günter Schlichthörl, Christian Derst, Andreas Karschin † and Jürgen Daut

Institute of Physiology, Marburg University, Deutschhausstrasse 2, 35037 Marburg and † Institute of Physiology, Würzburg University, Röntgenring 9, 97070 Würzburg, Germany

The two-pore-domain potassium channels TASK-1, TASK-3 and TASK-5 possess a conserved C-terminal motif of five amino acids. Truncation of the C-terminus of TASK-1 strongly reduced the currents measured after heterologous expression in *Xenopus* oocytes or HEK293 cells and decreased surface membrane expression of GFP-tagged channel proteins. Two-hybrid analysis showed that the C-terminal domain of TASK-1, TASK-3 and TASK-5, but not TASK-4, interacts with isoforms of the adapter protein 14-3-3. A pentapeptide motif at the extreme C-terminus of TASK-1, RRx(S/T)x, was found to be sufficient for weak but significant interaction with 14-3-3, whereas the last 40 amino acids of TASK-1 were required for strong binding. Deletion of a single amino acid at the C-terminal end of TASK-1 or TASK-3 abolished binding of 14-3-3 and strongly reduced the macroscopic currents observed in *Xenopus* oocytes. TASK-1 mutants that failed to interact with 14-3-3 isoforms (V411*, S410A, S410D) also produced only very weak macroscopic currents. In contrast, the mutant TASK-1 S409A, which interacts with 14-3-3-like wild-type channels, displayed normal macroscopic currents. Co-injection of 14-3-3ζ cRNA increased TASK-1 current in *Xenopus* oocytes by about 70 %. After co-transfection in HEK293 cells, TASK-1 and 14-3-3ζ (but not TASK-1ΔC5 and 14-3-3ζ) could be co-immunoprecipitated. Furthermore, TASK-1 and 14-3-3 could be co-immunoprecipitated in synaptic membrane extracts and postsynaptic density membranes. Our findings suggest that interaction of 14-3-3 with TASK-1 or TASK-3 may promote the trafficking of the channels to the surface membrane.

(Received 20 June 2002; accepted after revision 18 September 2002; first published online 27 September 2002)
Corresponding author J. Daut: Institute of Physiology, Marburg University,Deutschhausstrasse 2, 35037 Marburg, Germany.
Email: daut@mailer.uni-marburg.de

Two-pore-domain potassium channels (K_{2P} channels) are a family of potassium channels strongly expressed in the central nervous system (Talley *et al.* 2001) and characterized by very complex regulation (Lesage & Lazdunski, 2000; Goldstein *et al.* 2001; Patel *et al.* 2001). TASK-1 (*KCNK3*) (Duprat *et al.* 1997; Kim *et al.* 1999), TASK-3 (*KCNK9*) (Kim *et al.* 2000; Rajan *et al.* 2000) and TASK-5 (*KCNK15*) (Ashmole *et al.* 2001; Karschin *et al.* 2001; Kim & Gnatenco, 2001) are members of a subfamily of the K_{2P} channels. The defining property of the TASK (Two-pore-domain Acid Sensitive K^+ channel) subfamily is the inhibition of the trans-membrane K^+ currents by extracellular acidification (Duprat *et al.* 1997; Kim *et al.* 1999, 2000; Rajan *et al.* 2000). TASK-1 and TASK-3 are differentially expressed in the central nervous system, with high mRNA levels found in spinal cord motoneurons, in cerebellar granule cells and in neurons of the brain stem (Karschin *et al.* 2001; Talley *et al.* 2001). Recently it has been shown that in certain neurons TASK-1 and/or TASK-3 can be inhibited by activation of heptahelical receptors coupled to G proteins of the αq/11 subtype (Millar *et al.* 2000; Talley *et al.* 2000; Talley & Bayliss, 2002), and it has been suggested that K_{2P} channels are the likely effectors of slow excitatory postsynaptic potentials elicited by activation of metabotropic receptors. Transcripts of TASK-5 were found in olfactory bulb mitral cells and in cerebellar Purkinje cells, but were predominantly associated with central auditory pathways in the brain (Karschin *et al.* 2001). Since TASK-5 could not be functionally expressed in *Xenopus* oocytes (Ashmole *et al.* 2001; Karschin *et al.* 2001; Kim & Gnatenco, 2001) it has been speculated that surface membrane targeting of this channel requires an auxiliary subunit.

TASK channels, like other K_{2P} channels, possess a very short N-terminus and a relatively long C-terminus of 80–160 amino acids. The C-terminus of K_{2P} channels imparts regulatory properties such as sensitivity to volatile anaesthetics, membrane stretch, intracellular pH and arachidonic acid (Patel *et al.* 1999; Lesage & Lazdunski, 2000; Goldstein *et al.* 2001; Kim *et al.* 2001; Patel *et al.*

* These authors contributed equally to this work.

2001). In the present study we describe the interaction of the C-termini of TASK channels with members of the protein family 14-3-3. In mammals this family has seven members encoded by distinct genes. 14-3-3 proteins are differentially distributed in various tissues and are particularly abundant in the brain. They have been implicated in many cellular processes including regulation of protein kinases, cell cycle control, apoptosis and transfer of signalling molecules between nucleus and cytosol (Aitken, 1996; Benzing *et al.* 2000; Fu *et al.* 2000; Muslin & Xing, 2000; Shaw, 2000; Tzivion *et al.* 2001; van Hemert *et al.* 2001; Tzivion & Avruch, 2002).

Using yeast two-hybrid screens we found strong interaction of TASK-1, TASK-3 and TASK-5 with all mammalian isoforms of 14-3-3. After identifying a C-terminal pentapeptide that is essential for this interaction we tested whether surface membrane localisation of TASK channels and functional expression depended on the ability of the C-terminus to associate with 14-3-3. Experiments with various interacting and non-interacting mutants of TASK-1 revealed a close correlation between cell surface expression of the channel and its ability to associate with 14-3-3. Only channels capable of interacting with 14-3-3 were found to be localised at the surface cell membrane and gave rise to significant outward K^+ currents in the heterologous expression system. Furthermore, co-immunoprecipitation of the two proteins in brain extracts and postsynaptic density membranes showed that TASK channels and 14-3-3 can also interact in native cells. Taken together, our findings suggest that the interaction of TASK-1 with 14-3-3 is essential for efficient trafficking of the channels to the cell membrane. A preliminary communication of our findings has been published (Rajan *et al.* 2002).

METHODS

All experiments were carried out in accordance with the regional animal care committee guidelines (at the Regierungspräsidium Giessen, Germany). The temperature was 20–22 °C in all experiments. Results are presented as means ± S.E.M. Statistical significance was determined with Student's *t* test.

Yeast two-hybrid screen

The Matchmaker system (Clontech) was used for the screening of three libraries from rat brain (P-5), rat hippocampus (Hip) and rat embryonic tissues (E15) constructed in the yeast activation domain containing vector pGAD424. The C-terminal domains of rat (r) TASK-1 (aa 246–411), rTASK-3 (aa 249–397), human (h) TASK-5 (aa 247–330) and bovine (b) TASK-4 (aa 282–341; accession number AF479760) were amplified by PCR and cloned into the yeast DNA-binding domain-containing vector pGBT-9. The yeast strain HF7c was co-transformed with 100 μg vector and 50 μg library DNA and approximately 100 000 transformants were screened. Yeast colonies growing on 5 mM 3-aminotriazole plates were scored positive for interacting proteins. Strongly positive colonies appeared within 3 days, whereas weakly positive colonies appeared after 5 days. In addition, a β-galactosidase assay was performed to verify interaction. For checking the specific interaction between two proteins, 100 ng of both vectors was co-transformed.

Site-directed mutagenesis

For single amino acid replacement or deletion mutagenesis the QuikChange site-directed mutagenesis kit (Stratagene) was used. Oligonucleotide primers were designed with at least 10 matching nucleotides on each side of an intended nucleotide change. All mutants were completely sequenced.

Preparation of rat brain membrane fractions

Rat brain tissue was homogenised with a motor driven glass–Teflon homogeniser in ice-cold dissection buffer (50 mM Tris-acetate, pH 7.4, 10 % sucrose, 5 mM EDTA and freshly added protease inhibitor cocktail) and the cell debris was removed. Total membrane was collected by 100 000 *g* ultracentrifugation for 1 h and the pellet was re-suspended in 5 mM Tris-acetate with protease inhibitor cocktail (Sigma Aldrich). Synaptic membranes and postsynaptic density fractions were prepared by combined floatation and density gradient centrifugation (Rogers *et al.* 1991).

Co-immunoprecipitation and Western blotting

COS-7 or HEK293 cells were grown in DMEM and transfection was performed with 1–2 μg of DNA and 4 μl lipofectamine (Life Technologies). Transfected cells were harvested after 24 h and homogenised in ice-cold buffer containing 10 mM Hepes, 350 mM sucrose, 5 mM EDTA and protease inhibitor cocktail. Membranes were collected by centrifugation at 100 000 *g* for 1 h. Immunoprecipitation was performed with Dynabeads–Protein-A conjugates (Dynal) according to the manufacturer's instructions. Approximately 3 μg of the TASK-1 antibody (Alomone labs) was used for binding to 50 μl of Dynabeads–Protein-A conjugate, and a monoclonal mouse 14-3-3 antibody was used for detection. Immunoprecipitates or solubilised membrane proteins were resolved on 10 % (w/v) acrylamide gels and electroblotted to nitrocellulose membrane. Staining of the Western blot was done with 1:500 (for 14-3-3) or 1:2000 (for TASK-1) antibody dilution and nitroblue tetrazolium/5-bromo-4-chloro-3-indolyl phosphate (NBT/BCIP).

Fluorescence imaging

For fluorescence imaging and confocal microscopy, rTASK-1 and hTASK-3 were fused to the EGFP gene by cloning into the expression vector pEGFP-C1 (Clontech, Palo Alto, CA, USA) and images were taken 36–48 h after transfection of COS-7 cells with lipofectamine. Confocal fluorescence images were obtained via a × 60 oil-immersion objective lens (numerical aperture, 1.4) using a FV300 confocal system (Olympus, Hamburg, Germany). Laser intensity was set at 6 % and the pinhole was optimised for the × 60 objective. Conventional fluorescence images were obtained with a × 63 oil-immersion objective (numerical aperture, 1.2) using a Leica DMR microscope equipped with a SPOT CCD camera (INTAS Imaging Instruments, Göttingen, Germany). For comparison with EGFP-tagged channels, the surface membrane was labelled with the subcellular localisation vector pDsRED2-Mem, constructed by fusing the first 20 amino acids of rat neuromodulin (accession number NM017195) to the DsRed2 amino terminus, analogous to the pECFP-Mem from Clontech.

Voltage-clamp measurements in *Xenopus* oocytes

pEGFP-tagged TASK-1 constructs were cloned into the expression vector pSGEM. Capped run-off poly(A+) cRNA transcripts, purified using RNeasy mini columns (Qiagen, Hilden, Germany) and quantified photometrically, were injected individually or in combination into defolliculated oocytes at

constant amounts (~6 ng per oocyte). Oocytes were incubated at 19 °C in ND96 solution containing (mM): 96 NaCl, 2 KCl, 1 $MgCl_2$, 1 $CaCl_2$ and 5 Hepes (pH 7.4–7.5), supplemented with 100 μg ml^{-1} gentamicin and 2.5 mM sodium pyruvate. After 48 h incubation, two-microelectrode voltage-clamp measurements were performed with a Turbo Tec-10 C amplifier (npi, Tamm, Germany). Data were recorded via an EPC-9 interface at sampling rates up to 20 kHz using Pulse/Pulsefit software (HEKA). The oocytes were placed in a small-volume perfusion chamber and bathed in ND96 or in high-K^+ solution in which NaCl was replaced by equimolar KCl.

Single-channel measurements in HEK293 cells

HEK293 cells were co-transfected with 1–2 μg of rTASK-3 or rTASK-3ΔC5 cDNA and green fluorescent protein (GFP) in the pcDNA3.1 (Invitrogen) vector using lipofectamine 2000 (Life Technologies). Cell-attached single-channel measurements were carried out 24–36 h after transfection as described previously (Rajan *et al.* 2000; Liu *et al.* 2001) with a pipette solution containing (mM): 150 KCl, 10 EGTA and 10 Hepes (pH 7.3); and a bath solution containing (mM): 140 KCl, 1 $MgCl_2$, 1 $CaCl_2$, 0.33 NaH_2PO_4, 10 Hepes, 10 glucose (pH 7.4). Data acquisition was performed with an Axopatch 200B amplifier (Axon Instruments), an A/D converter (PCI-MIO 16-XE-10, National Instruments) and data acquisition and evaluation software developed in our laboratory (PC.DAQ 1.0) using LabView (National Instruments). The sampling rate was 15 kHz and the data were filtered with a −3dB cut-off frequency of 5 kHz. To avoid distortions due to the limited frequency resolution, unitary current amplitudes of 'flickery' channels were determined using an algorithm that excludes very short events. Analysis of open-time distribution of TASK channels was performed with an algorithm that allows reliable detection of current jumps four times larger than the standard deviation of the current signal produced by closed channels (~0.33 pA). The detection limit was set at 1.5 pA.

Whole-cell measurements in HEK293 cells

Whole-cell measurements in HEK293 cells were carried out with a pipette solution containing (mM): 65 potassium glutamate, 50 KCl, 10 KH_2PO_4, 7.9 $MgCl_2$, 5 EDTA, 5 Hepes, 1.9 K_2ATP and 0.2 Na_3GTP (pH 7.2); the bath contained (mM): 135 NaCl, 5 KCl, 1 $MgCl_2$, 1 $CaCl_2$, 0.33 NaH_2PO_4, 10 Hepes, 10 glucose (pH 7.4). Since the efficiency of transfection of HEK293 cells with lipofectamine varies form cell to cell in a Petri dish, quantitative comparison of current amplitudes after transient transfection with different channel mutants is notoriously difficult. To minimise the subjective factor involved in the selection of cells labelled more or less strongly with co-transfected GFP, the experiments were blinded and the nature of the transfected cDNA (wild-type or mutant) was revealed to the experimenter only after complete evaluation of the measurements.

RESULTS

C-terminal deletions of TASK-1 decrease whole-cell currents

The two-pore-domain K^+ channels TASK-1, TASK-3 and TASK-5 are highly homologous except for the cytosolic C-terminal domain, which is only weakly conserved. Nevertheless, several residues in the extreme C-terminal motif of five amino acids are identical in the three subfamily members (Fig. 1*A*). To clarify a possible functional role of the extreme C-terminus, we constructed several truncation mutants of rat (r) TASK-1 in which 1, 5, 20, 40 or 163 residues were removed from the cytosolic tail (ΔC1, ΔC5, ΔC20, ΔC40, ΔC163). For each construct the same amount of cRNA (determined photometrically) was injected into *Xenopus* oocytes. It was found that the whole-

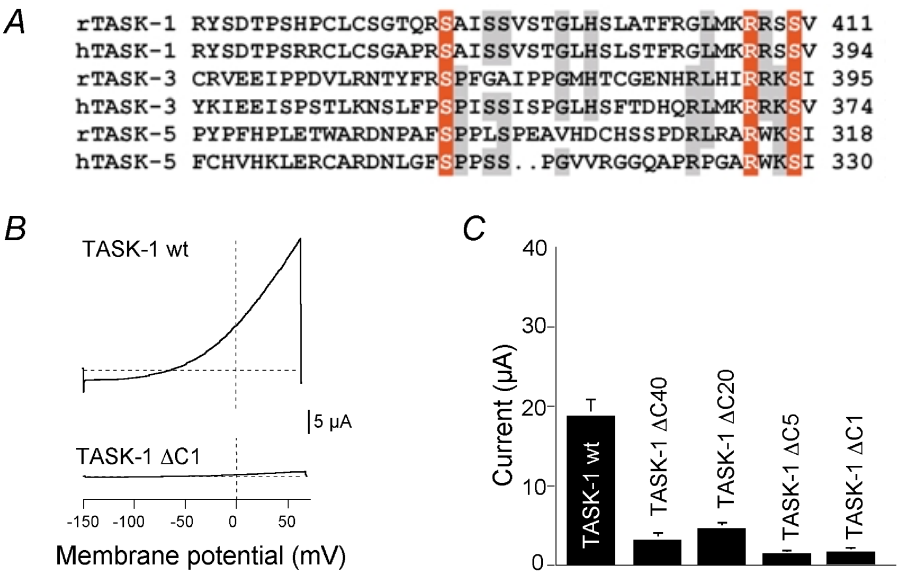

Figure 1. Expression of wild-type and truncated TASK channels in *Xenopus* oocytes

A, alignment of the last 43 amino acids of the C-terminus of rat (r) and human (h) TASK-1, TASK-3 and TASK-5. Conserved amino acids are represented in red and grey shades. *B*, whole-cell current–voltage relations measured in *Xenopus* oocytes for wild-type TASK-1 channels (wt) and truncated TASK-1 channels (ΔC) in which the C-terminal 40, 20, 5 or 1 amino acids were removed. Voltage ramps between −150 and +60 mV were applied. *C*, mean outward current measured at +30 mV for wt (n = 10) and truncated (n = 5 each) mutants.

Table 1. Comparison of currents recorded after transient expression of wild-type and truncated TASK-1 channels in *Xenopus* oocytes or HEK293 cells

	I_{mutant}	I_{wt}	I_{mutant} / I_{wt}
Oocytes, TASK-1ΔC1	1.48 ± 0.31 μA (10)	18.74 ± 1.67 μA (10)	0.08***
Oocytes, TASK-1ΔC5	1.25 ± 0.27 μA (10)	18.74 ± 1.67 μA (10)	0.07***
Oocytes, TASK-1ΔC20	4.64 ± 0.38 μA (10)	18.74 ± 1.67 μA (10)	0.25***
Oocytes, TASK-1ΔC40	3.11 ± 0.32 μA (10)	18.74 ± 1.67 μA (10)	0.17***
Oocytes, TASK-1ΔC163	0.58 ± 0.09 μA (10)	15.32 ± 1.34 μA (10)	0.04***
HEK293, TASK-1ΔC1	336 ± 98 pA (20)	1014 ± 208 pA (18)	0.33**
HEK293, TASK-1ΔC5	361 ± 60 pA (20)	741 ± 82 pA (24)	0.49***
HEK293, TASK-1ΔC163	287 ± 62 pA (19)	817 ± 96 pA (27)	0.35***

The number of cells from which the data were obtained is given in brackets. Statistical significance was calculated with Student's *t* test; ** $P < 0.01$; *** $P < 0.001$.

cell K^+ currents measured 24 h after injection of mutant cRNA were markedly reduced as compared to wild-type (wt) TASK-1 currents (Fig. 1*B* and *C*; Table 1).

Similar results were obtained in the mammalian cell line HEK293, as illustrated in Fig. 2. The cells were co-transfected with green fluorescent protein plus either wild-type or truncated rTASK-1 channels, and a blinded comparison of current amplitudes was carried out (see Methods). In three series of experiments we compared wild-type rTASK-1 with rTASK-1ΔC1, ΔC5 and ΔC163 (Table 1). We found that C-terminal truncation reduced the amplitude of TASK-1 currents in HEK293 cells, too, but the effects were significantly smaller than in *Xenopus* oocytes. This difference may be, at least partially, attributable to the technical limitations of the methods (see Discussion).

TASK channels interact with all isoforms of 14-3-3

To explore the possibility that the reduction in current amplitude may be related to specific protein–protein interactions we screened yeast two-hybrid libraries from adult rat brain (P5), rat hippocampus (Hip) and rat embryo (E15) with the hydrophilic C-terminal domains of rTASK-1 (amino acids 247–411), rTASK-3 (amino acids 249–397) and hTASK-5 (amino acids 247–330). Screening with the TASK-1 C-terminus yielded several isoforms of 14-3-3, a family of cytosolic adapter proteins: 14-3-3 *sigma* (σ, 2 clones from E15), *beta* (β, 1× E15, 2× Hip, 1 × P5), *theta* (θ, 2 × E5) and *zeta* (ζ, 1 × Hip). Screening with the TASK-3 C-terminus isolated 14-3-3 *beta* (1 × Hip) and *epsilon* (ϵ, 1 × Hip). TASK-5 C-terminus was found to interact with 14-3-3 *zeta* (5 × E15) and *epsilon* (2 × P5). Altogether five out of seven mammalian isoforms of 14-3-3 protein were isolated ($\sigma, \beta, \epsilon, \theta$ and ζ) in this way.

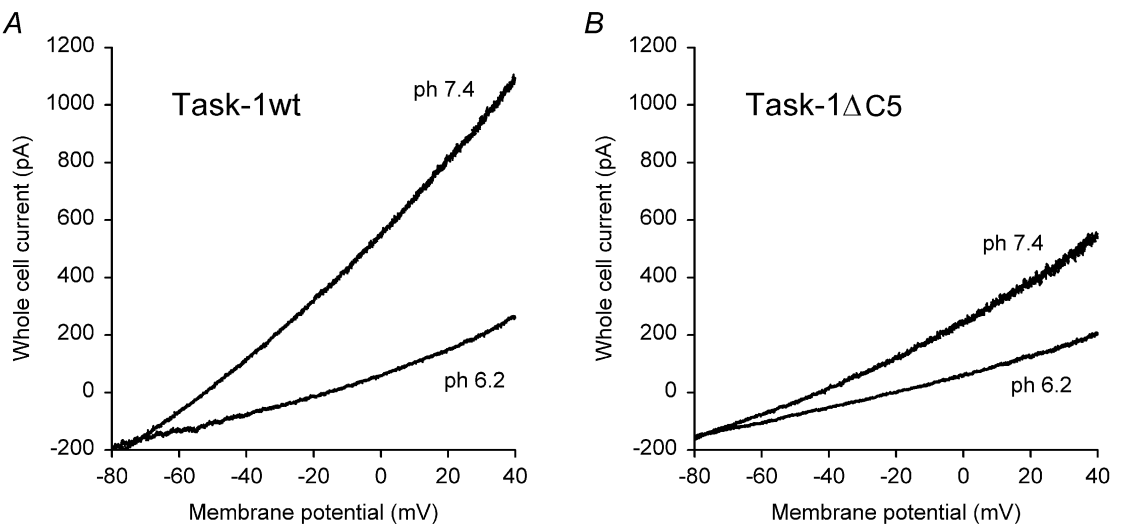

Figure 2. Expression of wild-type and truncated TASK channels in HEK293 cells

Representative recordings of whole-cell currents in HEK293 cells co-transfected with GFP and rTASK-1 (*A*) or with GFP and rTASK-1ΔC5 (*B*). The study was blinded as described in Methods.

We further analysed the interaction between the isoforms of 14-3-3 and the C-termini of TASK-1, TASK-3 and TASK-5 using specific two-hybrid interaction assays. As illustrated in Fig. 3, yeast strains co-transformed with the C-termini of K_{2P} channels (bait) and 14-3-3 isoforms (prey) show interaction-dependent growth in selective medium. The growth of red yeast colonies indicates interaction of 14-3-3 gamma (γ) with the complete C-terminus of TASK-3 (Fig. 3*A*) and TASK-1 (Fig. 3*B*). We found that all seven mammalian 14-3-3 isoforms, including 14-3-3 gamma (γ) and eta (η), can interact with the C-termini of TASK-1, TASK-3 and TASK-5. Figure 3*C* shows the qualitative score of the strength of interaction which was determined from the growth of colonies in 3-aminotriazole plates and from the intensity of colour development in the β-galactosidase assay. The interaction with 14-3-3 appears to be specific for the acid-sensitive K_{2P} subfamily comprising TASK-1, TASK-3 and TASK-5. The right-hand part of Fig. 3*A* shows that the mainly alkaline-sensitive K_{2P} channel TASK-4 did not interact with 14-3-3γ.

Dissection of the 14-3-3 binding domain

To identify the amino acid residues involved in 14-3-3 binding we constructed rTASK-1 C-terminal truncation mutants and tested their interaction with 14-3-3 in the yeast two-hybrid assay (Fig. 3*D*). First we noted that the fusion proteins containing either the complete C terminus (aa 246–411) or only the last 40 amino acids (aa 372–411) interacted with the 14-3-3 protein at equal strength. Further deletions, starting from the proximal part of the C-terminus, revealed a gradual decrease in binding strength. Interestingly, the construct containing the last five amino acids (RRSSV), but not that containing the last four amino acids, showed significant interaction with the 14-3-3 isoforms (Fig. 3*D*). Furthermore, a single amino acid deletion from the C-terminus (ΔC1; aa 246–410) was sufficient to completely disrupt the interaction (Fig. 3*B* and *D*). Taken together, the experiments illustrated in Fig. 3 indicate that a stretch of 40 amino acids in the TASK-1 C-terminus contributes to the binding of 14-3-3, whereas the terminal pentapeptide motif represents the essential 14-3-3 binding domain. The last four amino acids of TASK-1 (but not of TASK-3 and TASK-5) constitute a conserved PDZ binding motif (X-S/T-X-V/I), implicating an association with PDZ proteins such as PSD-95. However, the two-hybrid assay never detected interaction between the C-terminus of rTASK-1 and the conserved PDZ domain of PSD-95, nor was any PDZ protein isolated by screening the libraries with TASK C-termini.

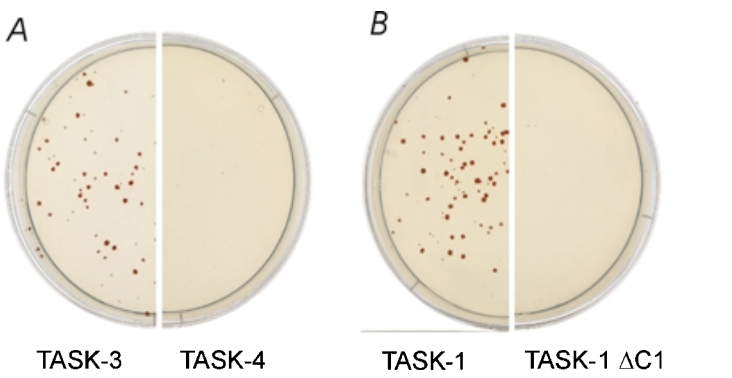

C

	γ	ζ	β	ε	θ	σ	η
TASK-1	++++	+++	++++	++	++	+	+++
TASK-3	++	++++	++	+	+	+	+++
TASK-5	++++	++++	++++	++	++	++++	+++

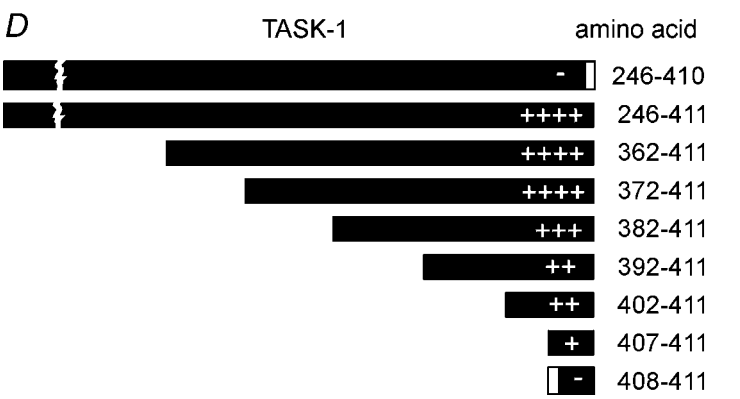

Figure 3. Specific yeast two-hybrid assays

A and *B*, typical examples of yeast two-hybrid analysis of the interaction between TASK channels and 14-3-3. Yeast strains co-transformed with the C-termini of TASK-3 (*A*) and TASK-1 (*B*) show strong growth in the selective medium. Co-transformation with the C-terminus of TASK-4 (*A*) and TASK-1 ΔC1 (*B*) showed no growth. *C*, yeast two-hybrid assay of the interaction of TASK channels with 14-3-3. The rating of the strength of interaction between the C-terminal domains of TASK-1, TASK-3 and TASK-5 (bait) and different isoforms of 14-3-3 (prey) is indicated. *D*, interaction of the C-terminus of rTASK-1 and of different deletion constructs with the ζ isoform of 14-3-3. The constructs are represented by boxes, the strength of interaction is indicated by the number of + signs. Symbols in *C* and *D*: ++++, interaction as strong as in the positive control (NMDA receptor and the PDZ protein PSD-95); +++, somewhat weaker than control; ++, distinctly weaker than control; +, positive; −, no growth of transformants.

Table 2. Growth of TASK-1 and TASK-5 constructs with single amino acid mutations (in the C-terminal pentapeptide motif) in histidine-deficient medium

TASK-1	*	A	G	I	K	R	T	W	Y
R-407	–	–	nt	nt	–		–	nt	–
R-408	–	–	–	–	–		–	–	–
S-409	–	++++	++++	++++	++++	++++	++++	nt	++++
S-410	–	–	–	–	–	–	++	–	–
V-411	–	nt	nt	++++	nt	nt	++++	nt	++++
TASK-5	*	A	G	D		R			
R -326	–	–	–	–					
W-327	–	nt	+	nt		++++			
K -328	–	++++	++++	++++		++++			
S -329	–	–	nt	–		nt			
I -330	–	++++	nt	++++		nt			

The residues indicated in the left column were either substituted by the amino acids or exchanged by a stop codon (designated as *). The strength of the interaction is indicated by the number of + signs: ++++, interaction as strong as in the positive control; +, positive; –, no growth of transformants observed; nt, not tested.

The essential C-terminal binding motif is RRx(S/T)x

To further characterise the structural determinants of the interaction with 14-3-3 we investigated the role of single amino acid residues in the terminal pentapeptide domain of rTASK-1 in detail. Two putative protein kinase A (PKA) phosphorylation sites are present within the last six amino acids of TASK-1 (KRRSSV) and one such site is present in TASK-3 (IRRKSI). We found that substitution of the arginine-407 of rTASK-1 by tyrosine, threonine, alanine or lysine, and replacement of arginine-408 by tyrosine, isoleucine, glycine, tryptophan or lysine completely disrupted the 14-3-3 binding (Table 2). Thus, the two arginine residues appear to be essential for the interaction with 14-3-3. Replacement of the serine at position 410 by threonine, but not by other amino acids, preserved the interaction with 14-3-3, suggesting that phosphorylation of the residue at position 410 may be required for 14-3-3 binding. Substitution of serine-409 of rTASK-1 by tyrosine, glycine, alanine or lysine and substitution of valine-411 by tyrosine or isoleucine did not disrupt the interaction with 14-3-3. Since the essential residues at positions 407, 408 and 410 are identical in TASK-1 and TASK-3, the C-terminal motif required for association of these channels with 14-3-3 appears to be RRx(S/T)x.

The C-terminal pentapeptide of TASK5 is RWKSI, thus lacking the arginine that is essential for 14-3-3 binding in TASK-1 and TASK-3. Interestingly, tryptophan 327 in hTASK-5 (corresponding to R408 in rTASK-1) is not essential for interaction. It could be replaced by arginine without affecting 14-3-3 binding (Table 2); with glycine at position 327 only weak binding was found. Despite these structural differences deletion of the very last amino acid (ΔC1) and substitution of the conserved serine at position-328 (corresponding to S409 in rTASK-1) also disrupted the binding of hTASK-5 to 14-3-3. Thus, the essential C-terminal pentapeptide for 14-3-3 binding to TASK-5 appears to be R(W/R)xSx.

Mutations in the interacting domain decrease K^+ current

Having characterised the pentapeptide motif essential for interaction between TASK channel proteins and 14-3-3 we tested how disruption of this motif affected TASK-1 currents in *Xenopus* oocytes. Identical amounts of wild-type or mutant TASK cRNA with single amino acid substitutions were injected in *Xenopus* oocytes and the amplitude of resulting macroscopic currents were compared. The mutants TASK-1 S410A, TASK-1 V411* (TASK-1ΔC1) and TASK-1 S410D (not shown), which disrupt the interaction, displayed only negligibly small whole-cell currents as compared to wild-type TASK-1 (Fig. 4*A* and *B*). On the other hand, the construct TASK-1 S409A, which disrupts the putative PDZ binding site but retains 14-3-3 binding, gave rise to macroscopic currents comparable to wild-type currents.

An analogous mutational analysis was carried out with the C-terminus of TASK-3 channels. Again we compared the current amplitudes of wild-type and mutant channels expressed in *Xenopus* oocytes. However, since TASK-3 channels show much stronger expression than TASK-1, we reduced the amount of wild-type cRNA by a factor of 10 as compared to mutant cRNA (to limit the maximal current amplitude). Even under these conditions the currents recorded after expression of mutant channels were greatly reduced in comparison to wild-type channels. Specific two-hybrid analysis showed that the three TASK-3 mutants tested (ΔC1, ΔC5, S394A), which are analogous to the TASK-1 mutants shown in Fig. 4*A* and *B*, did not interact with 14-3-3 (not illustrated). Thus, similar to TASK-1, expression of TASK-3 mutants incapable of interacting with 14-3-3 resulted in a markedly reduced current amplitude.

The biophysical characteristics of TASK-3 are not altered by C-terminal truncation

In principle, the reduction in TASK current could be due to impaired targeting of the mutant channels or to alteration of their biophysical characteristics. To clarify this issue we performed single-channel recordings in HEK293 cells transfected with wild-type TASK-3 or with TASK-3ΔC5 channels. Figure 5 shows typical cell-attached recordings of wild-type rTASK-3 (panel *A*) and TASK-3ΔC5 channels (panel *B*). We have shown previously that the single-channel current–voltage relation of guinea-pig TASK-3 channels shows inward rectification (Rajan *et al.*

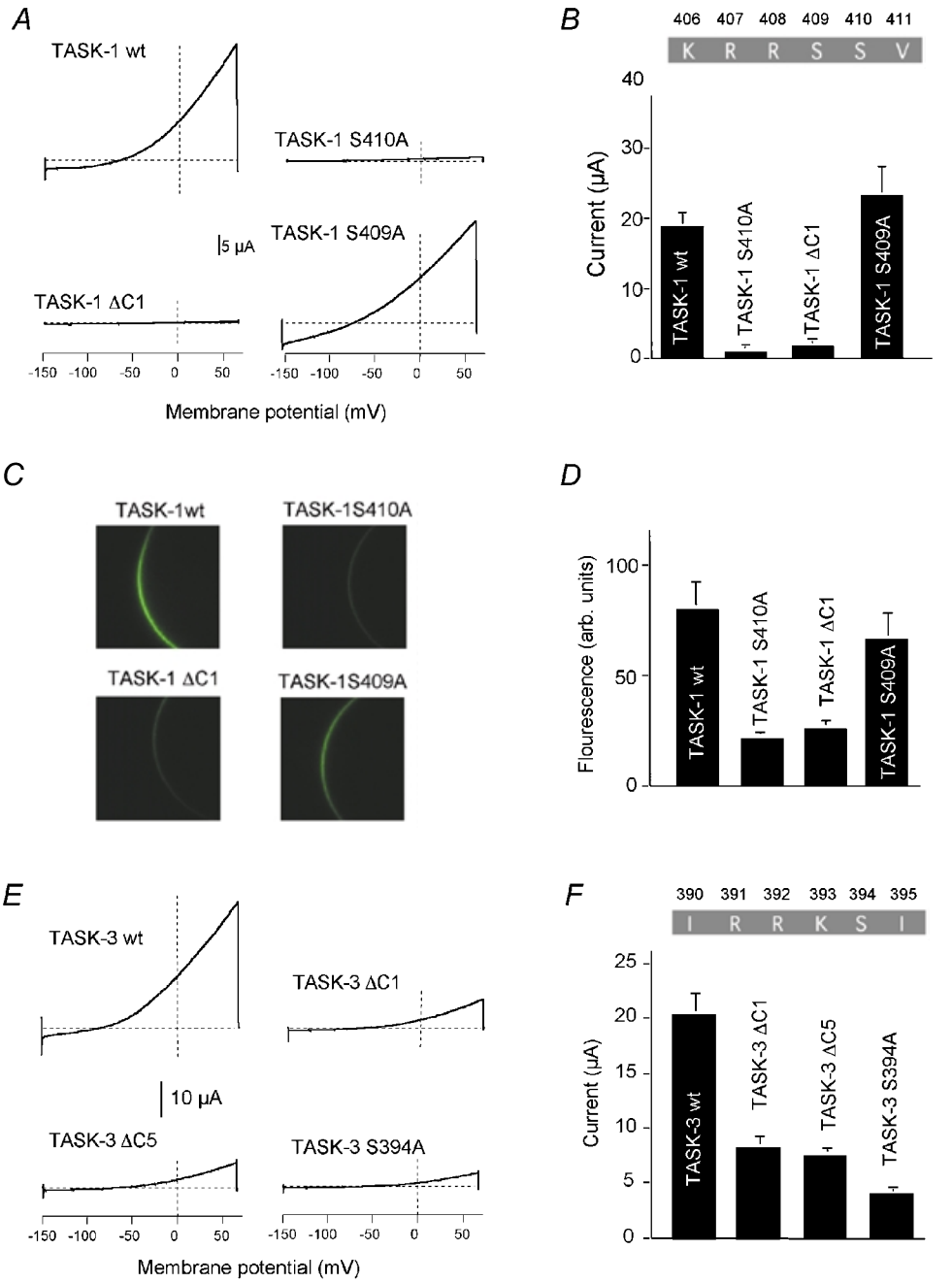

Figure 4. Macroscopic currents and surface expression of TASK channel mutants

A, typical macroscopic current measurement of wild-type TASK-1 and various mutants expressed in *Xenopus* oocytes. *B*, bar graph of results obtained from 5–10 oocytes for each construct. *C*, expression of EGFP-labelled TASK-1 constructs in *Xenopus* oocytes. The fluorescence of the cell membrane was measured 48 h after cRNA injection. *D*, comparison of the fluorescence intensity of different TASK-1 constructs, determined by line-scan luminometry (arbitrary units). *E*, typical macroscopic current measurement of wild-type TASK-3 and various mutants. *F*, bar graph of results obtained from 5–10 oocytes for each construct. The amount of wt TASK-3 cRNA injected was 10 times lower than that of mutant TASK-3 cRNA.

2000), and we have now confirmed this for rTASK-3 and rTASK-3ΔC5 (panel *E*). At transmembrane potentials between −60 and −100 mV the single-channel conductance was 136 ± 6 pS ($n = 7$) for wild-type rTASK-3 and 137 ± 9 pS ($n = 7$) for rTASK-3ΔC5, which is not significantly different.

The high resolution recordings shown in the lower traces of Fig. 5*A* and *B* and the all-point histograms depicted in Fig. 5*C* and *F* illustrate that the rapid kinetics of opening and closing of the channels could not be completely resolved. Nevertheless we were able to determine the mean open times in recordings showing no or only very few superimposed openings (Fig. 5*D* and *G*), as described in Methods. The mean open time was 0.164 ± 0.008 ms ($n = 8$) for rTASK-3 and 0.151 ± 0.004 ms ($n = 7$) for TASK-3ΔC5, which is not significantly different ($P > 0.05$). Taken together, these findings suggest that the biophysical properties of rTASK-3 channels were not altered by the truncation and that the observed changes in current amplitude were related to a reduction of the number of functional channels.

Disruption of 14-3-3 binding impairs transport to the surface membrane

EGFP-tagged rTASK-1 mutants were expressed in *Xenopus* oocytes to investigate localisation of the channels to the surface membrane. The mutants S410A, ΔC1 (Fig. 4*C* and *D*) and R407* (not shown), which are not capable of interacting with 14-3-3, demonstrated only faint plasma membrane fluorescence in *Xenopus* oocytes. In contrast, expression of the mutant S409A, which retains the 14-3-3 binding motif but not the putative PDZ binding motif, gave rise to a fluorescence intensity at the plasma membrane comparable to that of wild-type rTASK-1 (Fig. 4*C* and *D*).

As a second test of membrane localisation we compared the subcellular localisation of wild-type and mutant TASK-1 and TASK-3 channels in COS-7 cells. The cells were transfected with EGFP-tagged channels and confocal or conventional fluorescent images were taken 36–48 h later. Figure 6*A* and *B* shows representative examples of images taken 46 h after transfection of TASK-1 channels. Cells transfected with wild-type rTASK-1 showed distinct expression at the surface membrane (panel *A*). The

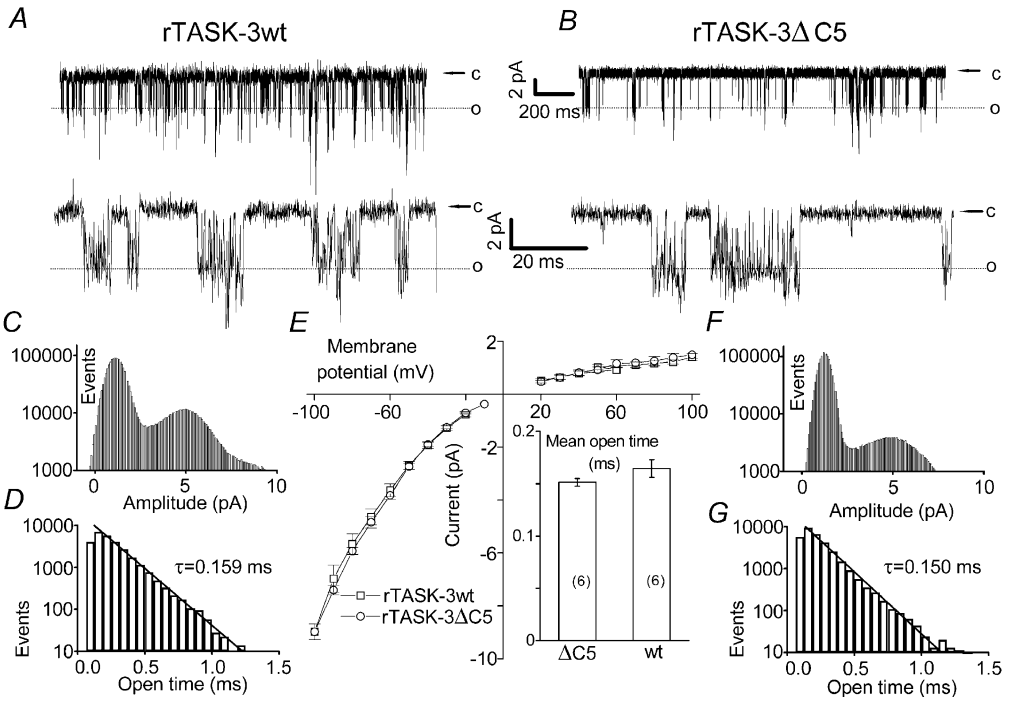

Figure 5. Single-channel recordings of wild-type and truncated TASK-3

A and *B*, typical cell-attached recordings of wild-type rTASK-3 (*A*) and rTASK-3ΔC5 (*B*) channels expressed in HEK293 cells (transmembrane potential, −60 mV). The lower traces show parts of the record at higher time resolution. *C* and *F*, typical all-point histograms showing the number of data points per 0.08 pA bin. *D* and *G*, typical open time distributions (sampling rate, 15 kHz). *E*, single-channel current–voltage relation of wt rTASK-3 and rTASK-3ΔC5 ($n = 7$ each). The conductance was estimated by applying a linear fit to the data points obtained between – 60 and – 100 mV for individual channels. The inset shows the mean open times wt rTASK-3 and rTASK-3ΔC5 ($n = 6$ each). The recordings shown in *A*, *C* and *D* were from the same wt TASK-3 channel; the recordings shown in *B*, *F* and *G* were from the same rTASK-3ΔC5 channel.

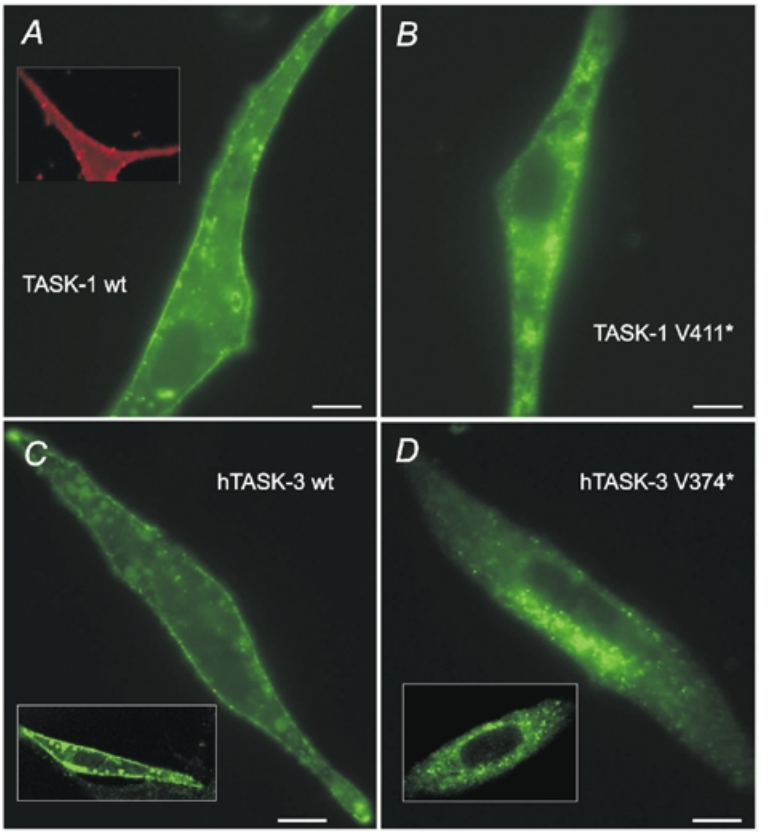

Figure 6. Subcellular localisation of TASK channels in COS-7 cells

A, conventional fluorescence image of EGFP-tagged wild-type rTASK-1 taken 46 h after transfection. The inset shows confocal images of a plasma membrane marker fused to DsRed2. *B*, image of rTASK-1 V411* taken under the same conditions as in panel *A*. *C*, conventional fluorescence image and confocal image (inset) of wild-type hTASK-3. *D*, conventional fluorescence image and confocal image (inset) of hTASK-3 V374*. All images depicted in *C* and *D* were taken 36 h after transfection. The scale bars are 10 μm.

localisation was confirmed by comparison with the membrane marker pDsRED2-Mem (inset). In contrast, after deletion of the terminal amino acid (rTASK-1 V411*) the fluorescence was mainly localised in the cytoplasm. Close inspection by eye revealed very weak or undetectable labelling of the surface membrane. Similar results were obtained 36 h after transfection of COS-7 cells with EGFP-tagged hTASK-3 channels. Figure 6*C* shows that transfection with wild-type hTASK-3 clearly labelled the surface membrane. The membrane localisation could be seen even more clearly in the confocal images, as illustrated in the inset. In contrast, after transfection of the EGFP-tagged hTASK-3 V374* mutant (removal of the C-terminal valine) fluorescence was mainly seen in the cytoplasm, with occasional very weak labelling of the surface membrane (Fig. 6*D*). This result was confirmed by confocal images taken under very similar conditions, as illustrated in the inset. The results presented in Fig. 6*A–D* are representative; more than 90 % of the cells transfected with wild-type or mutant channels showed the typical localisation depicted here.

Overexpression of 14-3-3 increases TASK-1 currents. 14-3-3 proteins are strongly expressed in most cells and are especially abundant in brain, but the cell-specific distribution of the isoforms is still unclear. To test whether

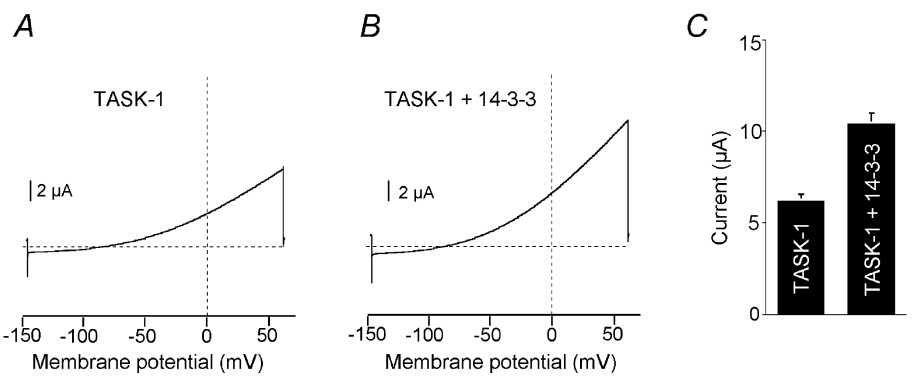

Figure 7. Overexpression of 14-3-3 in *Xenopus* oocytes

A and *B*, typical measurement of whole-cell currents after injection of TASK-1 cRNA. *A*, injection of 2 ng TASK-1 cRNA only, control. *B*, co-injection of TASK-1 cRNA (2 ng) and 14-3-3ζ cRNA (4 ng). *C*, bar graph of results obtained from 10 oocytes in each group.

14-3-3 might be involved in post-translational regulation of channel expression we investigated the effect of overexpression of 14-3-3 on the density of TASK-1 currents in *Xenopus* oocytes. Injection of 2 ng TASK-1 cRNA produced a TASK current with an amplitude of 6.2 ± 0.4 μA (n = 10) at +30 mV, as illustrated in Fig. 7. When, in addition, 4 ng of 14-3-3ζ cRNA was co-injected the resulting TASK-1 current increased to 10.4 ± 1.3 μA (n = 10), which is significantly different ($P < 0.01$). Thus it was possible to increase the surface expression of functional TASK-1 channels above the level established by endogenous 14-3-3 proteins. These findings are consistent with the idea that the interaction with 14-3-3 proteins may play a role in the posttranslational regulation of assembly and/or trafficking of TASK channels.

Co-immunoprecipitation of TASK-1 and 14-3-3. Next we investigated whether interaction between TASK channels and 14-3-3 also occurs *in vivo*. Figure 8*A* shows immunostaining of extracts from native cells. In extracts from rat brain (lane 2), as well as in synaptic membrane (syn. m., lane 3) and in post synaptic density (PSD) fractions (lane 4) a distinct 50 kDa TASK-1 protein was detected. This protein was ~5 kDa larger than the TASK-1 protein detected in heart extracts (lane 1), possibly due to post-translational modification. A 30 kDa fraction of 14-3-3 was also present in heart extracts and was abundant in all rat brain fractions (Fig. 8*B*). The specificity of the TASK-1 antibodies was tested using membranes of transfected HEK293 cells (Fig. 8*C*). In Western blots from HEK293 cells transfected with GFP plasmids, no immunosignal could be detected with the anti-TASK-1 antibody (lane 1). In contrast, after transfection with both GFP and TASK-1 plasmids, a double band between 40 and 44 kDa was seen (lane 2), possibly due to phosphorylation of the channel protein. The same membrane extract showed no immunosignal when the anti-TASK-1 antibody was competitively inhibited with its antigenic peptide (lane 3).

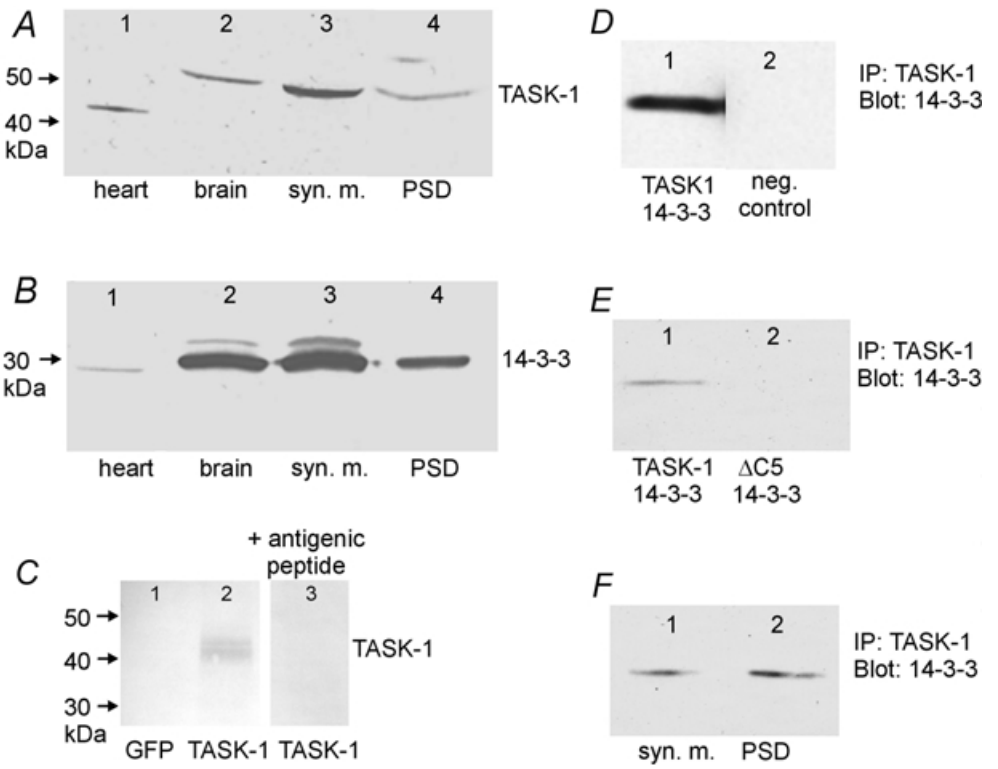

Figure 8. Detection of TASK-1 and 14-3-3 immunoreactivity with specific antibodies

A and *B*, Western blot of membrane extracts from native cells. *A*, the 42–45 kDa band in heart (lane 1) corresponds to the cardiac TASK-1 isoform; the 50 kDa band in lanes 2–4 corresponds to the brain TASK-1 isoform detected with a TASK-1-specific polyclonal antibody. *B*, 14-3-3 was detected in all samples with a monoclonal antibody that recognises all seven isoforms of 14-3-3. *C*, Western blot of membrane extracts of HEK293 cells transfected with GFP alone (lane 1), or with both GFP and TASK-1 (lanes 2 and 3). All lanes were stained with anti-TASK-1 antibody; in lane 3 the antibody was competitively inhibited with its antigenic peptide (1 μg peptide per 1 μg antibody). *D*, co-precipitation of 14-3-3 with a TASK-1 specific antibody in lysates of HEK293 cells transfected with TASK-1 and 14-3-3. The precipitates were detected with a 14-3-3 antibody (lane 1). The negative control (lane 2) was carried out with non-transfected cells. *E*, co-precipitation of 14-3-3 with a TASK-1 specific antibody from lysates of HEK293 cells transfected with 14-3-3 plus TASK-1 (lane 1) or with 14-3-3 plus TASK-1ΔC5 (lane 2). *F*, co-precipitation of 14-3-3 in a rat brain synaptic membrane fraction (lane 1) and in a postsynaptic density fraction (lane 2) with a TASK-1-specific antibody.

To determine whether TASK-1 forms a complex with 14-3-3, HEK293 cells were transfected with TASK-1 and 14-3-3ζ, TASK-1 was immunoprecipitated from the cell lysate with a specific antibody, and the precipitate was probed with a 14-3-3 antibody. As shown in Fig. 8*D*, a specific 14-3-3 antibody recognised the TASK-1 immunoprecipitate. Figure 8*E* shows co-immunoprecipitation experiments carried out with lysates of HEK293 cells transfected with 14-3-3 plus either TASK-1 or TASK-1ΔC5. TASK-1 was immunoprecipitated and the precipitate was probed with a 14-3-3 antibody that recognised all isoforms. It was found that 14-3-3 was co-immunoprecipitated with rTASK-1, but not with rTASK-1ΔC5.

To test whether this interaction also occurs *in vivo*, rat synaptic membrane extracts and postsynaptic density membranes were immunoprecipitated with the TASK-1 antibody and probed with the 14-3-3 antibody. Figure 8*F* shows that the antibody recognised endogenous 14-3-3 both in the synaptic membrane extract and in the PSD fraction. These results indicate that rTASK-1 is closely associated with 14-3-3 isoforms, both in transfected cell lines and in native cells, and confirm the idea that the pentapeptide motif in the C-terminal tail of TASK-1 is required for this interaction to take place.

DISCUSSION

Two-hybrid analysis revealed strong interaction between TASK-1, TASK-3 and TASK-5 and members of the protein family 14-3-3. Using truncated TASK-1 C-termini as bait and 14-3-3ζ as prey we have shown that the last 40 amino acids of the C-terminal tail contribute to the interaction between the channel and 14-3-3 and that the pentapeptide motif RRx(S/T)x is essential for the interaction. The most striking finding was that deletion of a single amino acid at the C-terminus of TASK-1 or TASK-3 (ΔC1) disrupted (i) the interaction with 14-3-3, (ii) the expression of functional currents in *Xenopus* oocytes, and (iii) the surface localisation of EGFP-tagged channels in *Xenopus* oocytes. Furthermore, we have shown that only those mutants of TASK-1 or TASK-3 which interacted with 14-3-3 in the two-hybrid assay produced a significant outward current in *Xenopus* oocytes, and that the same mutants, tagged with EGFP, produced membrane fluorescence in *Xenopus* oocytes similar to wild-type channels. Taken together, these results suggest that interaction with 14-3-3 promotes functional expression of TASK-1 and TASK-3 channels. The finding that overexpression of 14-3-3ζ increased TASK-1 current in *Xenopus* oocytes by ~70 % raises the possibility that isoforms of 14-3-3 may be involved in post-translational regulation of channel expression, for example, by participating in channel assembly in the endoplasmic reticulum or by modulating trafficking, retention or retrieval of TASK channel proteins.

In the other expression system used, the mammalian cell line HEK293, C-terminal truncation of TASK-1 was also associated with a reduction in acid-sensitive outward current, but the effects were significantly smaller (Table 1). The reduction in current amplitude was probably not related to a change in single-channel conductance or open probability since the biophysical properties of truncated TASK-3 channels (which can be analysed more precisely than the properties of TASK-1 channels) were found to be unaltered. Removal of the entire C-terminus at residue 248 (rTASK-1ΔC 163) reduced the current amplitude to about 35 % in HEK293 cells and to about 4 % in *Xenopus* oocytes. In agreement with other groups, who used this mutant to study the regulation of TASK-1 (Patel *et al.* 1999; Maingret *et al.* 2001; Talley & Bayliss, 2002), we found that the 'residual' macroscopic current of truncated TASK-1 channels in HEK293 cells showed characteristics similar to wild-type TASK-1 (pH sensitivity, coupling to heptahelical receptors).

We interpret these findings to indicate that after transient transfection a fraction of the truncated mutants may escape the quality control mechanisms in the endoplasmic reticulum, giving rise to qualitatively normal currents in HEK (or COS) cells. Another possible complication is that with sufficient overexpression the density of wild-type channels expressed in mammalian cell lines may reach saturation. The combination of these effects may lead to an underestimation of the effects of interacting proteins on the functional expression of ion channels. Thus, transient transfection of mammalian cell lines is a suitable approach for studying biophysical properties, signal transduction and subcellular localisation of ion channels. However, in our hands injection of known quantities of cRNA into *Xenopus* oocytes (which can synthesise very large amounts of protein) allowed a more precise quantification of the functional expression of different channel mutants. The consistent results obtained with both expression systems and with both channels, TASK-1 and TASK-3, support the idea that interaction with 14-3-3 may play an important role in the assembly and/or the trafficking of TASK channel proteins to the surface membrane.

This conclusion is substantiated by our confocal imaging and co-immunoprecipitation experiments in mammalian cells. Only wild-type TASK-1, but not TASK-1ΔC5, was co-immunoprecipitated with 14-3-3 in extracts of co-transfected HEK293 cells. Furthermore, GFP-tagged wild-type rTASK-1 and hTASK-3 channels were clearly targeted to the cell membrane of COS-7 cells, whereas the corresponding ΔC1 mutants showed much weaker labelling of the surface membrane. Finally, co-immunoprecipitation of TASK-1 and 14-3-3 was found in rat synaptic membrane extracts and postsynaptic density membranes, indicating that interaction between 14-3-3 and TASK channels also occurs *in vivo*.

The pentapeptide motif RRx(S/T)x that is essential for 14-3-3 binding to TASK-1 represents a consensus PDZ binding site. However, two-hybrid analysis of the interaction between TASK-1 and PSD-95 gave negative results, whereas the interaction between NMDA receptor and PSD-95 (used as control) was strongly positive. Furthermore, the construct TASK-1 S409A, which disrupted the putative PDZ binding site but retained 14-3-3 binding, gave rise to macroscopic currents and surface membrane fluorescence comparable to those of wild-type. TASK-3 and TASK-5 do not posses a consensus PDZ binding motif. Thus it is rather unlikely that PDZ binding is involved in the localisation of TASK channels to the surface membrane.

The tertiary structure of 14-3-3 monomers and dimers has been elucidated recently (Dubois *et al.* 1997; Yaffe *et al.* 1997; Rittinger *et al.* 1999; Obsil *et al.* 2001). It is now clear that all 14-3-3 isoforms have an amphipathic phosphoprotein binding pocket and a dimer contact surface lined primarily by hydrophobic residues. Stable association of most molecular partners with 14-3-3 requires formation of a 14-3-3 homo- or heterodimer (Tzivion *et al.* 2000; Tzivion & Avruch, 2002). Most of the regulatory mechanisms of 14-3-3 proteins depend on their binding to specific phosphoserine-containing sequence motifs (subdivided into mode 1 and mode 2 binding sites; Tzivion & Avruch, 2002) and require phosphorylation of the central serine in the binding domain. The essential 14-3-3 binding domain reported here, RRx(S/T)x, also contains an S/T phosphorylation site, but it does not agree with either mode 1 or mode 2 consensus motifs (Yaffe *et al.* 1997; Rittinger *et al.* 1999; Tzivion & Avruch, 2002) since it lacks the terminal proline.

The experiments reported here raise the issue of how the interaction between TASK channels and 14-3-3 may govern surface localisation. Our working hypothesis is that the association of 14-3-3 with TASK-1 or TASK-3 is required to enable the binding of an accessory protein (motor protein, β-subunit or chaperone) that facilitates trafficking of the assembled dimeric channel proteins from the endoplasmic reticulum to the surface membrane. Alternatively, the binding of 14-3-3 may mask a retention/retrieval motif and thus prevent the binding of an accessory protein that mediates retention in the endoplasmic reticulum. Either of these mechanisms would efficiently modulate the number of TASK-1 channels reaching the surface membrane. Our conclusion that binding of 14-3-3 to the C-terminus of TASK-1 strongly enhances surface membrane targeting should not be taken to imply that this interaction is sufficient to promote membrane targeting. It may well be that dimeric 14-3-3 proteins also interact with other cytosolic domains of TASK-1 (for example with M2–M3-linker or with the cytosolic N-terminus), as has recently been shown for the K^+ channel HERG (Kagan *et al.* 2002). Thus, it is also possible that both mechanisms mentioned here play a role in determining the subcellular localisation of TASK-1 and TASK-3.

Our two-hybrid analysis indicates that 14-3-3 interacts with the hTASK-5 C-terminus as strongly as with the C-termini of TASK-3 and TASK-1. Nevertheless, binding of endogenous 14-3-3 is apparently not sufficient to cause surface membrane targeting of hTASK-5 in *Xenopus* oocytes (Ashmole *et al.* 2001; Karschin *et al.* 2001; Kim & Gnatenco, 2001). Analysis of chimeric TASK-5/TASK-3 constructs (Karschin *et al.* 2001) suggests that the failure of functional expression of TASK-5 may be related to an additional retention motif (or a binding site for an accessory protein) localised between the M1 and the M3 region.

K^+ channels control excitability, action potential waveforms and firing patterns of neuronal cells. Each population of neurons expresses a specific set of K^+ channels, resulting in distinct input/output characteristics. The open probability of most K^+ channels can be modulated by neurotransmitters which activate G-protein coupled receptors and mobilise intracellular second messengers. Recently it has been found that the gene expression of different subtypes of K^+ channels may also be subject to regulation (Levitan & Takimoto, 1998), and that the resulting change in outward current amplitude is associated with profound changes in neuronal function (Liss *et al.* 2001). Furthermore, both the functional properties and the density of channels in the surface membrane can be modulated at the post-transcriptional level by glycosylation and by interaction with β-subunits or anchoring proteins (Rettig *et al.* 1994; Shi *et al.* 1996; Yang *et al.* 2001; Tanemoto *et al.* 2002). The results presented here describe a novel mechanism of post-transcriptional regulation of K^+ channel density. Variable (possibly phosphorylation dependent) interaction with different isoforms of 14-3-3 may represent a mechanism for regulating the assembly and/or the trafficking of TASK channels to the surface membrane. The resulting variation in K^+ conductance is expected to alter the input/output characteristics of neuronal cells and may thus play a role in the dynamic regulation of information processing in the central nervous system.

REFERENCES

Aitken, A. (1996). 14-4-4 and its possible role in coordinating multiple signalling pathways. *Trends in Cell Biology* **6**, 341–347.

Ashmole, I., Goodwin, P. A. & Stanfield, P. R. (2001). TASK-5, a novel member of the tandem pore K^+ channel family. *Pflügers Archiv* **442**, 828–833.

Benzing, T., Yaffe, M. B., Arnould, T., Sellin, L., Schermer, B., Schilling, B., Schreiber, R., Kunzelmann, K., Leparc, G. G., Kim, E. & Walz, G. (2000). 14-3-3 interacts with regulator of G protein signaling proteins and modulates their activity. *Journal of Biological Chemistry* **275**, 28167–28172.

Dubois, T., Howell, S., Amess, B., Kerai, P., Learmonth, M., Madrazo, J., Chaudhri, M., Rittinger, K., Scarabel, M., Soneji, Y. & Aitken, A. (1997). Structure and sites of phosphorylation of 14-3-3 protein: role in coordinating signal transduction pathways. *Journal of Protein Chemistry* **16**, 513–522.

Duprat, F., Lesage, F., Fink, M., Reyes, R., Heurteaux, C. & Lazdunski, M. (1997). TASK, a human background K^+ channel to sense external pH variations near physiological pH. *EMBO Journal* **16**, 5464–5471.

Fu, H., Subramanian, R. R. & Masters, S. C. (2000). 14-3-3 proteins: structure, function, and regulation. *Annual Review of Pharmacology and Toxicology* **40**, 617–647.

Goldstein, S. A., Bockenhauer, D., O'Kelly, I. & Zilberberg, N. (2001). Potassium leak channels and the KCNK family of two-P-domain subunits. *Nature Reviews Neuroscience* **2**, 175–184.

Kagan, A., Melman, Y. F., Krumerman, A. & McDonald, T. V. (2002). 14-3-3 amplifies and prolongs adrenergic stimulation of HERG K^+ channel activity. *EMBO Journal* **21**, 1889–1898.

Karschin, C., Wischmeyer, E., Preisig-Muller, R., Rajan, S., Derst, C., Grzeschik, K. H., Daut, J. & Karschin, A. (2001). Expression pattern in brain of TASK-1, TASK-3, and a tandem pore domain K^+ channel subunit, TASK-5, associated with the central auditory nervous system. *Molecular and Cellular Neuroscience* **18**, 632–648.

Kim, D. & Gnatenco, C. (2001). TASK-5, a new member of the tandem-pore K^+ channel family. *Biochemical and Biophysical Research Communications* **284**, 923–930.

Kim, Y., Bang, H., Gnatenco, C. & Kim, D. (2001). Synergistic interaction and the role of C-terminus in the activation of TRAAK K^+ channels by pressure, free fatty acids and alkali. *Pflügers Archiv* **442**, 64–72.

Kim, Y., Bang, H. & Kim, D. (1999). TBAK-1 and TASK-1, two-pore K^+ channel subunits: kinetic properties and expression in rat heart. *American Journal of Physiology* **277**, H1669–1678.

Kim, Y., Bang, H. & Kim, D. (2000). TASK-3, a new member of the tandem pore K^+ channel family. *Journal of Biological Chemistry* **275**, 9340–9347.

Lesage, F. & Lazdunski, M. (2000). Molecular and functional properties of two-pore-domain potassium channels. *American Journal of Physiology – Renal Physiology* **279**, F793–801.

Levitan, E. S. & Takimoto, K. (1998). Dynamic regulation of K^+ channel gene expression in differentiated cells. *Journal of Neurobiology* **37**, 60–68.

Liss, B., Franz, O., Sewing, S., Bruns, R., Neuhoff, H. & Roeper, J. (2001). Tuning pacemaker frequency of individual dopaminergic neurons by Kv4.3L and KChip3.1 transcription. *EMBO Journal* **20**, 5715–5724.

Liu, G. X., Derst, C., Schlichthörl, G., Heinen, S., Seebohm, G., Brüggemann, A., Kummer, W., Veh, R. W., Daut, J. & Preisig-Müller, R. (2001). Comparison of cloned Kir2 channels with native inward rectifier K^+ channels from guinea-pig cardiomyocytes. *Journal of Physiology* **532**, 115–126.

Maingret, F., Patel, A. J., Lazdunski, M. & Honore, E. (2001). The endocannabinoid anandamide is a direct and selective blocker of the background K^+ channel TASK-1. *EMBO Journal* **20**, 47–54.

Millar, J. A., Barratt, L., Southan, A. P., Page, K. M., Fyffe, R. E., Robertson, B. & Mathie, A. (2000). A functional role for the two-pore domain potassium channel TASK-1 in cerebellar granule neurons. *Proceedings of the National Academy of Sciences of the USA* **97**, 3614–3618.

Muslin, A. J. & Xing, H. (2000). 14-3-3 proteins: regulation of subcellular localization by molecular interference. *Cellular Signalling* **12**, 703–709.

Obsil, T., Ghirlando, R., Klein, D. C., Ganguly, S. & Dyda, F. (2001). Crystal structure of the 14-3-3zeta:serotonin N-acetyltransferase complex: A role for scaffolding in enzyme regulation. *Cell* **105**, 257–267.

Patel, A. J., Honore, E., Lesage, F., Fink, M., Romey, G. & Lazdunski, M. (1999). Inhalational anesthetics activate two-pore-domain background K^+ channels. *Nature Neuroscience* **2**, 422–426.

Patel, A. J., Lazdunski, M. & Honore, E. (2001). Lipid and mechano-gated 2P domain K^+. channels. *Current Opinion in Cell Biology* **13**, 422–428.

Rajan, S., Presig-Müller, R., Nehring, R., Wischmeyer, E., Karschin, A., Daut, J. & Derst, C. (2002). A C-terminal pentapeptide motif interacting with 14-3-3 protein strongly enhances cell surface expression of TASK-1, a 2P domain K^+ channel. *Biophysical Journal* **82**, 201a–202a (abstract).

Rajan, S., Wischmeyer, E., Xin Liu, G., Preisig-Müller, R., Daut, J., Karschin, A. & Derst, C. (2000). TASK-3, a novel tandem pore domain acid-sensitive K^+ channel. An extracellular histidine as pH sensor. *Journal of Biological Chemistry* **275**, 16650–16657.

Rettig, J., Heinemann, S. H., Wunder, F., Lorra, C., Parcej, D. N., Dolly, J. O. & Pongs, O. (1994). Inactivation properties of voltage-gated K^+ channels altered by presence of beta-subunit. *Nature* **369**, 289–294.

Rittinger, K., Budman, J., Xu, J., Volinia, S., Cantley, L. C., Smerdon, S. J., Gamblin, S. J. & Yaffe, M. B. (1999). Structural analysis of 14-3-3 phosphopeptide complexes identifies a dual role for the nuclear export signal of 14-3-3 in ligand binding. *Molecular Cell* **4**, 153–166.

Rogers, S. W., Hughes, T. E., Hollmann, M., Gasic, G. P., Deneris, E. S. & Heinemann, S. (1991). The characterization and localization of the glutamate receptor subunit GluR1 in the rat brain. *Journal of Neuroscience* **11**, 2713–2724.

Shaw, A. (2000). The 14-3-3 proteins. *Current Biology* **10**, R400.

Shi, G., Nakahira, K., Hammond, S., Rhodes, K. J., Schechter, L. E. & Trimmer, J. S. (1996). Beta subunits promote K^+ channel surface expression through effects early in biosynthesis. *Neuron* **16**, 843–852.

Talley, E. M. & Bayliss, D. A. (2002). Modulation of TASK-1 (Kcnk3) and TASK-3 (Kcnk9) potassium channels. Volatile anesthetics and neurotransmitters share a molecular site of action. *Journal of Biological Chemistry* **277**, 17733–17742.

Talley, E. M., Lei, Q., Sirois, J. E. & Bayliss, D. A. (2000). TASK-1, a two-pore domain K^+ channel, is modulated by multiple neurotransmitters in motoneurons. *Neuron* **25**, 399–410.

Talley, E. M., Solorzano, G., Lei, Q., Kim, D. & Bayliss, D. A. (2001). CNS distribution of members of the two-pore-domain (KCNK) potassium channel family. *Journal of Neuroscience* **21**, 7491–7505.

Tanemoto, M., Fujita, A., Higashi, K. & Kurachi, Y. (2002). PSD-95 mediates formation of a functional homomeric Kir5.1 channel in the brain. *Neuron* **34**, 387–397.

Tzivion, G. & Avruch, J. (2002). 14-3-3 proteins: active cofactors in cellular regulation by serine/threonine phosphorylation. *Journal of Biological Chemistry* **277**, 3061–3064.

Tzivion, G., Luo, Z. J. & Avruch, J. (2000). Calyculin A-induced vimentin phosphorylation sequesters 14-3-3 and displaces other 14-3-3 partners in vivo. *Journal of Biological Chemistry* **275**, 29772–29778.

Tzivion, G., Shen, Y. H. & Zhu, J. (2001). 14-3-3 proteins; bringing new definitions to scaffolding. *Oncogene* **20**, 6331–6338.

van Hemert, M. J., Steensma, H. Y. & van Heusden, G. P. (2001). 14-3-3 proteins: key regulators of cell division, signalling and apoptosis. *Bioessays* **23**, 936–946.

Yaffe, M. B., Rittinger, K., Volinia, S., Caron, P. R., Aitken, A., Leffers, H., Gamblin, S. J., Smerdon, S. J. & Cantley, L. C. (1997). The structural basis for 14-3-3:phosphopeptide binding specificity. *Cell* **91**, 961–971.

Yang, E. K., Alvira, M. R., Levitan, E. S. & Takimoto, K. (2001). Kvbeta subunits increase expression of Kv4.3 channels by interacting with their C termini. *Journal of Biological Chemistry* **276**, 4839–4844.

Acknowledgements
This work was supported by the Deutsche Forschungsgemeinschaft (grants Da 177/7-3, Ka 1175/1-3 and Da 177/8-1), the Ernst-and-Berta-Grimmke Stiftung and the P. E. Kempkes-Stiftung.